

Four decades of water quality change in the upper San Francisco Estuary[†]

Marcus W. Beck,^{*,‡} David Senn,[¶] Thomas Jabusch,[¶] and Phil Trowbridge[¶]

[‡]*USEPA National Health and Environmental Effects Research Laboratory, Gulf Ecology*

Division, Gulf Breeze, FL

[¶]*San Francisco Estuary Institute, Richmond, CA*

E-mail: beck.marcus@epa.gov

Phone: +1 (850)9342480. Fax: +1 (850)9342401

Abstract

Recent methods for trend analysis have been developed that leverage the descriptive potential of multi-decadal monitoring data. We apply an estuarine adaptation of the Weighted Regressions on Time, Discharge, and Season (WRTDS) model to describe water quality trends over four decades in the Delta region of the San Francisco Estuary (SFE). Results from multiple stations in the Delta provided novel descriptions of historical trends and relationships between key species of dissolved inorganic nitrogen (ammonium, nitrate/nitrite, total). Trend analysis with WRTDS flow-normalized data demonstrated the potential to misinterpret changes using observed data that include flow effects, such that several trends with flow-normalized data had changes in magnitude and even reversal of trends relative to the observed. We further demonstrate use of WRTDS to provide insight into mechanisms of change with two case studies that 1) evaluate downstream changes in nitrogen following upgrades at a wastewater

{acro:wrtds}

{acro:sfe}

[†]Version: Wed Jan 18 13:48:31 2017 -0600, [49568114dc54151cfc21515b651815124b3db256](#)

treatment plant, and 2) effects of biological invasion on chlorophyll dynamics in Suisun Bay. Overall, this analysis provides an ecological and management-based understanding of historical trends in the Delta as a means to interpret potential impacts of recent changes and expected trends.

1 Introduction

Trend analysis is a broad discipline that has been applied to time series for the interpretation of environmentally-relevant changes. Direct evaluation of an observed time series is often insufficient given that a long-term change can be masked by variation at shorter time scales or the observed variation represents the combined effects of many variables.^{1,2} Climate, local, regional, and historical effects may act individually or together to impose a change on time series, such that methods that account for variation at different scales have been used for trend analysis.³⁻⁶ As a practical approach for water quality evaluation, trend analysis of eutrophication endpoints often focuses on tracking the change in concentrations or loads of nutrients over many years. Indicators of eutrophication can vary naturally with changing flow conditions and may also reflect long-term effects of management or policy changes. For example, chlorophyll *a* (chl-*a*) concentration as a measure of phytoplankton response to nutrient inputs can follow seasonal patterns with cyclical variation in temperature and light changes throughout each year, whereas annual trends can follow long-term variation in nutrient inputs to the system.^{7,8} Similarly, nutrient trends that vary with hydrologic loading also vary as a function of utilization rates by primary producers or decomposition processes.⁹⁻¹¹ Time series analysis of water quality indicators must simultaneously consider effects of processes at multiple scales and interactions between variables of interest to develop a more comprehensive description of system change.

Appropriate methods for the analysis of change depend largely on the question of interest and on characteristics of the environmental dataset. Trend analyses for aquatic systems have traditionally focused on comparisons between discrete periods of time to estimate a

direction and magnitude of a trend using non-parametric tests.^{12,13} Development of these conventional approaches addressed limitations in historical monitoring datasets related to infrequent sampling and relatively few years of continuous data. Increased availability of multi-decadal datasets, particularly for high profile environments, has accelerated development of trend analysis methods that leverage the descriptive potential of long-term time series from continuous monitoring programs.^{6,14} These methods are often data-driven where the parameterization of a simple functional model can change smoothly over time given that relationships between water quality variables and potential drivers are dynamic. The Weighted Regressions on Time, Discharge, and Season (WRTDS) approach was developed under this context and has been used to characterize decadal trends in running-water systems.¹⁵⁻¹⁹ This method has the potential to provide a spatially and temporally robust description of trends by fitting a dynamic model with parameters that change relative to the domain of interest. More recently, the WRTDS method was adapted for trend analysis in tidal waters, with a focus on chl-*a* trends in Tampa Bay²⁰ and the Patuxent River Estuary,²¹ and tidally-influenced time series of dissolved oxygen from continuous sonde measurements.²² These studies have demonstrated the potential of WRTDS for trend analysis in tidal waters and further application to alternative datasets could provide additional insight into eutrophication dynamics in aquatic systems.

The San Francisco Estuary (SFE) on the Pacific Coast of the United States is one of the most prominent and culturally significant estuaries in the western hemisphere.²³ Background nutrient concentrations in the Bay often exceed those associated with excessive primary production, although eutrophication events have historically been infrequent. Recent changes in response to additional stressors (e.g., variation in freshwater inputs/withdrawals, invasive species, climate change) suggests that Bay condition has not followed past trajectories and more subtle spatial and temporal variation could provide clues that describe underlying properties of this system.²⁴ The unique ecological and social context of the Bay provides a valuable opportunity to gain insight into ecosystem properties of estuaries that define water

quality dynamics at different scales. The Delta region of SFE in particular is a mosaic of inflows that receives and processes inputs from the larger watershed to the lower Bay.^{25–27} A comprehensive monitoring dataset has been collected at several fixed locations in the Delta for the last four decades.²⁸ Moreover, nutrient dynamics in the Delta are inherently linked to flow variation from inputs, withdrawal, impoundments, and downstream transport,²⁹ suggesting an approach that explicitly considers flow effects is critical for trend analysis. To date, the Delta monitoring dataset is an under-utilized data source and a comprehensive analysis with WRTDS could facilitate an understanding of historical and recent changes in SFE water quality.

The goal of this study was to provide a comprehensive description of nutrient trends in the Delta to inform understanding of eutrophication dynamics and potential causes of water quality change in the larger Bay. We applied the newly-adapted method of weighted regression for tidal waters to describe nitrogen trends in different spatial and temporal contexts. The specific objectives were to 1) quantify and interpret trends over four decades at ten stations in the Delta, including annual, seasonal, and spatial changes in nitrogen analytes and response to flow variation, and 2) provide detailed descriptions of two case studies in the context of conceptual relationships modelled with WRTDS. The second objective evaluated two specific water quality stations in the Delta to demonstrate complexities with nutrient response to flow, effects of nutrient-related source controls on ambient conditions, and effects of biological invasion by benthic filter feeders on primary production. Although quantitative descriptions of change can be ends in themselves, the results provide a means to more detailed understanding of ecosystem properties. Products derived from WRTDS can be used to inform additional analyses, such as water quality response after removing annual, seasonal, or flow effects.

2 Materials and Methods

2.1 Study system

The SFE drains a 200 thousand km² watershed and is the largest bay on the Pacific coast of North America. The watershed provides drinking water to over 25 million people, including irrigation for 18 thousand km² of agricultural land in the Central Valley. Water enters the Bay through the Sacramento and San Joaquin rivers that have a combined inflow of approximately 28 km³ per year, with the Sacramento accounting for 84% of inflow to the Delta. The SFE system is divided into several sub-bays, including Suisun Bay immediately downstream of the Delta, San Pablo Bay to the north, South Bay, and the Central Bay that drains to the Pacific Ocean through the Golden Gate. Water dynamics in SFE are governed by inflows from the watershed, tidal exchange with the Pacific Ocean, and water withdrawals for municipal and agricultural use.²⁵ Seasonally, inflows into SFE peak in the spring and early summer from snowmelt in the upper watershed, whereas consumption, withdrawals, and export have steadily increased from 1960 to present but vary considerably depending on inter-annual climate effects.²⁴ The system is mixed mesotidal and significant exchange with the ocean occurs daily, although the extent of landward saltwater intrusion varies with inflow and annual water use patterns. Notable drought periods have occurred from 1976-1977, 1987-1992, and recently from 2013-2015.²³ Oceanic upwelling and climatic variation are also significant external factors that have influenced water quality dynamics in the Bay.³⁰

Nutrient loading in SFE is comparable to other large estuaries that exhibit symptomatic effects of cultural eutrophication (e.g., Chesapeake Bay).³¹ Orthophosphate (PO_4^{3-}) and dissolved inorganic nitrogen (DIN) enter the Bay primarily through riverine sources in the north and municipal wastewater treatment plant (WWTP) inputs in the densely-populated area immediately surrounding SFE. Annual nutrient export from the Delta region has been estimated as approximately 30 thousand kg d⁻¹ of total nitrogen (varying with flow²⁹), with

90% of ammonium (NH_4^+) originating solely from the Sacramento Regional WWTP.²⁷ Although nitrogen and phosphorus inputs are considerable, primary production is relatively low and not nutrient-limited.^{26,32} The resistance of SFE to the negative effects of eutrophication has historically been attributed to the unique physical and biological characteristics of the Bay, including strong tidal mixing that limits stratification^{7,33} and limits on phytoplankton growth from high turbidity and filter-feeding by bivalve mollusks.^{33,34} However, recent water quality trends have suggested that resistance of the system to nutrient inputs is decreasing given documented changes in chlorophyll biomass,³⁰ increased occurrence of hypoxic conditions,³⁵ and increased abundance of phytoplankton species associated with harmful algal blooms.^{36,37} These recent changes have been attributed to variation in global sea surface temperatures associated with climate change,³⁰ biological invasions,³⁸ and departures from the historical flow record.^{24,39} The role of nutrients in stimulating primary production in SFE has been the focus of several recent investigations.^{40–42}

The Delta region is of particular interest for understanding historical patterns and potential trajectories of water quality response to nutrient inputs into the Bay (Figure 1). The Delta is a mosaic of linked channels or tracts that receive, process, and transport inflows from the Sacramento and San Joaquin rivers.^{25,27,29} Quantitative descriptions of nutrient dynamics in the Delta are challenging given multiple sources and the volume of water that is exchanged through the system with natural and anthropogenic processes. A comprehensive evaluation using mass-balance models to describe nutrient dynamics in the Delta demonstrated that nitrogen enters the system in different forms and is processed at different rates before export or removal.²⁹ For example, a majority of ammonium entering the system during the summer is nitrified or assimilated, whereas a considerable percentage of total nitrogen load to the Delta is lost. Although, the focus of our analysis is not to quantify sources or sinks of nitrogen species, a quantitative evaluation of long-term trends will provide a more comprehensive historical interpretation to hypothesize the effects of future changes in the context of known dynamics. Nutrients in the Delta also vary with seasonal and annual changes in the delivery

of water inflows, including water exports directly from the system.^{25,27} Our analysis also explicitly accounts for the effects of flow changes on nutrient response to better understand variation both within the Delta and potential mechanisms of downstream transport.

2.2 Data sources

Multi-decadal time series of nutrients and flow records were used to develop a quantitative description of nitrogen trends in the Delta. The Interagency Ecological Program (IEP) is a consortium of state and federal agencies that have maintained the Environmental Monitoring Program (EMP) in the Delta region since 1975.⁴³ The EMP collects monthly water quality samples at 19 stations in the Delta, Suisun Bay, and northeastern San Pablo Bay. Water samples were collected using a Van Dorn sample, a submersible pump, or a flow through system depending on site. All samples were processed with standard QA/QC at the California Department of Water Resources Bryte Laboratory in Sacramento.⁴³ Nutrient time series were obtained from the IEP website (<http://water.ca.gov/bdma/meta/Discrete/data.cfm>) at ten discrete sampling stations from 1976 through 2013 (Figure 1). Stations were grouped by location in the study area for comparison: Delta stations C3 (Sacramento inflow), C10 (San Joaquin inflow), MD10, P8; middle stations D19, D26, D28; and Suisun stations D4, D6, and D7. These stations were chosen based on continuity of the water quality time series and geographic location for understanding trends. Time series were complete for all stations except for an approximate ten year gap from 1996-2014 for D19. Data were minimally processed with the exception of averaging replicates that occurred on the same day. The three nitrogen analytes that were evaluated were ammonium, nitrite/nitrate, and DIN (as the sum of the former two). Less than 3% of all observations were left-censored, although variation was observed between analytes and location. The ammonium time series had the most censored observations at sites C10 (25.4% of all observations), MD10 (18.1%), D28 (17.8%), D19 (12%), and D7 (7.9%).

Daily flow estimates for the Delta region were obtained from the Dayflow software pro-

gram that provides estimates of average Delta outflow.⁴⁴ Because of the complexity of water inflow, exports, and outflows from the Delta, the Dayflow program combines observations with estimates based on mass balance to reconstruct historical and daily flow estimates. The WRTDS models described below require a matched flow record with the appropriate station to evaluate nutrient trends. Given the complexity of inflows and connectivity of the system, only the inflow estimates from the Sacramento and San Joaquin rivers were used as measures of freshwater influence at each station. Initial analyses indicated that model fit was not significantly improved with flow estimates from locations closer to each station, nor was model fit improved using lagged times series. As such, the Sacramento daily flow time series was used to account for flow effects at C3, D19, D26, D28, and MD10, and the San Joaquin time series was used for C10 and P8 based on station proximity to each inflow. Salinity observations at D4, D6, and D7 in Suisun Bay were used as more appropriate measures of freshwater variation given the stronger tidal influence at these stations. Salinity has been used as a tracer of freshwater influence for the application of WRTDS models in tidal waters.²⁰

2.3 Analysis method and application

A total of thirty WRTDS models were created, one for each nitrogen analyte at each station. The functional form of WRTDS is a simple regression¹⁵ that models the log-transformed response variable as a function of time, flow, and season:

$$\ln(N) = \beta_0 + \beta_1 t + \beta_2 \ln(Q) + \beta_3 \sin(2\pi t) + \beta_4 \cos(2\pi t) \quad (1)$$

where N is one of three nitrogen analytes, time t is a continuous variable as decimal time to capture the annual or seasonal trend, and Q is the flow variable (either flow or salinity depending on station). The seasonal trend is modelled as a sinusoidal component to capture periodicity between years. The WRTDS model is a moving window regression that fits

unique parameters at each observation point in the time series. A unique set of weights is used for each regression to control the importance of observations used to fit the model relative to the observation at the center of the window. The weights are based on a scaled Euclidean distance to estimate the differences of all points from the center in relation to annual time, season, and flow. The complete model for the time series contains a parameter set for every time step that considers the unique context of the data. As such, predictions from WRTDS are more precise than those from more conventional models that fit a single parameter set to the entire time series.^{20,45} The WRTDS model applied to the Delta time series was based on a tidal adaptation of the original method.²⁰ The WRTDS models were fit to describe the conditional mean response using a weighted Tobit model for left-censored data.⁴⁶ Previous adaptations of WRTDS to tidal waters have used quantile regression to describe trends in the conditional quantiles, such as changes in the frequency of occurrence of extreme events. The application to the Delta data focused only on the conditional mean models to establish a baseline response which has not been previously quantified. All analyses used the WRTDStidal package written by the authors for the R statistical programming language.^{47,48}

A hallmark of the WRTDS approach is the description of flow-normalized trends that are independent of variation from freshwater inflows. Although variation in nutrients can be caused by the combined effects of several variables acting at different temporal and spatial scales, flow-normalization provides a basis for further exploration by removing a critical confounding variable that could affect the interpretation of trends. A flow-normalized value is the average of predictions at a given observation using all flow values that are expected to occur for the relevant month across years in the record. Flow-normalized trends for each analyte at each station were used to describe long-term changes in different annual and seasonal periods. Specifically, flow-normalized trends in each analyte were summarized as both medians and percent changes from the beginning to end of annual groupings from 1976-1995 and 1996-2013, and seasonal groupings of March-April-May (spring), June-July-August

(summer), September-October-November (fall), and December-January-February (winter) within each annual grouping. These annual and seasonal groupings were chosen for continuity with similar comparisons reported in Ref. 28 and as approximate twenty year midpoints in the time series.

Trends in each annual and seasonal grouping were based on seasonal Kendall tests of the flow-normalized predictions. This test is a modification of the non-parametric Kendall test that accounts for variation across seasons in the response variable.⁴⁹ Results from the test can be used to evaluate the direction, magnitude, and significance of a monotonic change within the period of observation. The estimated rate of change per year is also returned as the Theil-Sen slope and was interpreted as the percent change per year when divided by the median value of the response variable in the period of observation.²⁷ Trends in annual groupings were based on all monthly observations within relevant years, whereas seasonal groupings were based only on the relevant months across years. Seasonal Kendall tests were also used to describe trends in the observed data. These trends were compared with those based on the flow-normalized trends to evaluate the improved ability of WRTDS to describe trends that are independent of flow. Functions in the EnvStats package in R were used for the seasonal Kendall tests.⁵⁰

3 Results and Discussion

3.1 Observed Data

The observed time series for the ten Delta stations had substantial variation in scale among the nitrogen analytes and differences in apparent seasonal trends (Figure S1). In general, long-term (inter-annual) trends were not easily observed from the raw data. DIN for most stations was dominated by nitrite/nitrate, whereas ammonium was a smaller percentage of the total. However, C3 had a majority of DIN composed of ammonium and other stations (e.g., P8, D26) had higher concentrations of ammonium during winter months when phyto-

plankton assimilation is lower.²⁹ By location, observed concentrations of DIN for the entire time series were higher on average for the upper Delta stations (C3, C10, MD10, P8; maximum likelihood estimation of mean \pm standard error: 1.04 ± 0.03 mg L⁻¹) and similar for the middle (D19, D26, D28, 0.43 ± 0.01) and Suisun Bay stations (D4, D6, D7, 0.44 ± 0.01). Average concentrations were highest at P8 (1.63 ± 0.05 mg L⁻¹) and lowest at C3 (0.4 ± 0.01) for DIN, highest at P8 (0.28 ± 0.02) and lowest at D28 (0.05 ± 0.003) for ammonium, and highest at C10 (1.4 ± 0.04) and lowest at C3 (0.15 ± 0.004) for nitrite/nitrate. Mean observed concentrations were also higher later in the time series for all analytes. For example, average DIN across all stations was 0.61 ± 0.01 mg L⁻¹ for 1976-1995, compared to 0.7 ± 0.01 for 1996-2013. Seasonal changes across all years showed that nitrogen concentrations were generally lower in the summer and higher in the winter, although observed patterns were inconsistent between sites. For example, site MD10 had distinct seasonal spikes for elevated DIN in the winter, whereas other stations had less prominent variation between years (D6, D7, Figure S1).

3.2 Trends

Application of seasonal Kendall tests to evaluate trends in observed data provided explicit information on the direction, magnitude, and statistical significance of changes between years. Trends estimated from the observed data for 1976-1995 and 1996-2013 varied considerably between sites and analytes (Figure 2). Significant trends were observed from 1976-1995 for eight of ten sites for DIN (seven increasing, one decreasing), eight sites for ammonium (six increasing, two decreasing), and six sites for nitrite/nitrate (five increasing, one decreasing). More sites had decreasing trends for the observed data from 1996-2013. Eight sites had significant trends for DIN (four increasing, four decreasing), seven sites for ammonium (five increasing, two decreasing), and eight sites for nitrite/nitrate (four increasing, four decreasing). Trends by location (upper Delta, middle, and Suisun stations) were not apparent, suggesting individual sites had trends that differed independent of relative location. For

example, P8 had a relatively large decrease in ammonium (-8.3% change per year) for the second annual period compared to all other sites. Trends by season were similar such that increases were generally observed in all seasons from 1976-1995 (Figure S2) and decreases were observed for 1996-2013 (Figure S3). Trends for the seasonal comparisons were noisier and significant changes were less common compared to the annual comparisons.

Relationships between flow and observed water quality are complex and can change significantly through space and time.^{15,19} These principles have been demonstrated for monitoring data in the Delta region,²⁷⁻²⁹ suggesting that trend analyses using the observed time series are confounded by flow effects. As a proof of concept, Figure 3 demonstrates use of WRTDS to isolate a flow-normalized time series from the observed DIN data at C10. Raw data are presented in Figure 3a and the annual results by water year (October through September) from WRTDS are shown in Figure 3b. In addition to removing the seasonal component, Figure 3b shows the flow-normalized component (solid line) independent of the model predictions. The difference between predicted and flow-normalized results is shown in Figure 3c, such that years with predictions greater or less than the flow-normalized values correspond with long-term trends in flow shown in Figure 3d. For example, 1984 is a period of high flow and a large, negative difference between prediction and flow-normalized concentration, suggesting a dilution effect of increased flow on nutrients. Further, Figure 3e shows WRTDS estimates of seasonal variation in the relationships of DIN with flow throughout the period of record. Increases in flow (y-axis) were associated with an increase in DIN (colors) for flow values within the observed range. Seasonal patterns also differed throughout the time period with a wider range of DIN within a growing season in the early 2000s relative to the 1980s, which is potentially linked to long-term climatic patterns.³⁰

A comparison of trends with flow-normalized results from WRTDS relative to observed data is justified because flow and nutrient concentrations were linked at many of the stations in the study area, similar to Figure 3. These comparisons are made to identify changes in the magnitude, significance, and direction of trends, all of which have important implications

for decision-making. For all sixty trend comparisons in Figure 2 (flow-normalized values in Table S1) regardless of site, nitrogen analyte, and time period, thirteen comparisons had trends that were insignificant with the observed data but significant with flow-normalized results, whereas only one trend changed to insignificant. This suggests that time series that include flow effects have sufficient noise to obscure or prevent identification of an actual trend of a water quality parameter. Further, changes in the magnitude of the estimated percent change per year were also apparent for the flow-normalized trends, such that fourteen comparisons showed an increase in magnitude (more negative or more positive) and twenty five had a decrease (less positive or less negative) compared to observed trends. Eleven comparisons showed a trend reversal from positive to negative estimated change and ten sites went from no change to negative estimated trends for the flow-normalized results. Differences by season in the observed relative to flow-normalized trends from WRTDS were also apparent (Figures S2 and S3 and Tables S2 and S3). The most notable changes were an overall decrease in the estimated trend for most sites in the summer and fall seasons for 1996-2013, including an increase in the number of statistically significant trends.

Differences in apparent trends underscore the importance of considering flow effects in the interpretation of environmental changes., particularly if trend evaluation is used to assess the effects of nutrients on ecosystem health or the effectiveness of past nutrient management actions. Our results demonstrated the potential to misinterpret trends if flow effects are not considered, where the misinterpretation could vary from a simple change in the magnitude and significance of a trends, to more problematic changes where the flow-normalized trend could demonstrate a complete reversal relative to the observed. A more comprehensive evaluation of flow in the Delta demonstrated that flow contributions of different end members vary considerably over time at each station.²⁹ For example, flow at MD10 represents a changing percentage by season of inputs from the Sacramento, San Joaquin, Cosumnes, Mokelumne rivers, and agricultural returns. For simplicity, water quality observations in our analyses were matched with large-scale drivers of flow into the Delta where most sites

were matched to Sacramento or San Joaquin daily flow estimates. Given that substantial differences with flow-normalized results were apparent from relatively coarse estimates of flow contributions, more precise differences could be obtained by considering the influence of multiple flow components at each location. Output from the Dayflow software program⁴⁴ provides a complete mass balance of flow in the Delta that could be used to develop a more comprehensive description of flow-normalized trends that considers changing contributions over time.

3.3 Selected examples

Two stations were chosen to demonstrate use of WRTDS to develop a more comprehensive description of decadal trends in the Delta. The selected case studies focused on 1) effects of wastewater treatment upgrades upstream of P8, and 2) effects of biological invasion on nutrient dynamics in Suisun Bay using observations from D7. Each case study is built around hypotheses that results from WRTDS models were expected to support, both as a general description and for additional testing with alternative methods.

3.3.1 Effects of wastewater treatment

Significant efforts have been made in recent years to reduce nitrogen loading from regional WWTPs given the disproportionate contribution of nutrients relative to other sources (e.g., watershed agricultural load, sediment flux, etc.)^{29,51} Several WWTPs in the Delta have recently been or are planned to be upgraded to include tertiary filtration and nitrification to convert biologically available ammonium to nitrate. The City of Stockton WWTP was upgraded in 2006 and is immediately upstream of station P8 (Figure 1),²⁸ which provides a valuable opportunity to assess how nutrient or nutrient-related source controls and water management actions have changed ambient concentrations downstream. A modal response of nutrient concentrations at P8 centered around 2006 is expected as a result of upstream WWTP upgrades, and water quality should exhibit 1) a shift in nutrient contributions from

the WWTP before/after upgrade, and 2) a flow-normalized annual trend at P8 to show a change concurrent with WWTP upgrades.

Effluent concentrations measured from 2003 to 2009 from the Stockton WWTP showed a gradual reduction in ammonium concentration relative to the total (Figure S4). Ammonium and nitrate concentrations were generally balanced prior to 2006, whereas nitrate was a majority of total nitrogen after the upgrade with much smaller percentages from ammonium and nitrite. As expected, flow-normalized nitrogen trends at P8 shifted in response to upstream WWTP upgrades (Figure 4a), with ammonium showing an increase from 1976 followed by a large reduction in the 2000s. Interestingly, nitrite/nitrate concentrations also showed a similar but less dramatic decrease despite an increase in the WWTP effluent concentrations following the upgrade. Percent changes from seasonal Kendall tests on flow-normalized results showed that both nitrogen species increased prior to WWTP upgrades (2% per year for nitrite/nitrate, 2.8% for ammonium), followed by decreases after upgrades (−1.9% for nitrite/nitrate, −16.6% for ammonium, Table 1). Seasonally, increases prior to upgrades were highest in the summer for nitrite/nitrate (2.4%) and in the fall for ammonium (4.9%). Similarly, seasonal reductions post-upgrade were largest in the summer for nitrite/nitrate (−4.3%) and largest for ammonium in the winter (−26.7%).

Relationships of nitrogen with flow described by WRTDS showed an inverse flow and concentration dynamic with flushing or dilution at higher flow (Figure 4b). Seasonal variation was more apparent for ammonium, although both typically had the highest concentrations at low flow in the winter (January). Additionally, strength of the flow/nutrient relationship changed between years. Nitrite/nitrate typically had the strongest relationship with flow later in the time series (i.e., larger negative slope), whereas ammonium had the strongest relationship with flow around 2000 in January. Using WRTDS, an empirical link is created between upstream changes and observed effects downstream that is characterized by differences in analytes between years and season. A general conclusion is that ammonium reductions were concurrent with WWTP upgrades, but the reduction was most apparent at

low-flow in January. These dynamics are difficult to characterize from the observed time series, and further, results from WRTDS can be used to develop additional hypotheses of factors that influence nutrient concentrations at P8. For example, estimated ammonium concentrations in July were low for all flow levels which suggests either nitrogen inputs were low in the summer or nitrogen was available and uptake by primary consumers was high. Seasonal patterns in the relationship between flow and nitrite/nitrate were not as dramatic as compared to ammonium, and in particular, low-flow events in July were generally associated with higher concentrations. This could suggest that ammonium concentrations at P8 are driving phytoplankton production at low flow during warmer months, and not nitrite/nitrate given the higher estimated concentrations in July at low flow. As such, these simple observations from WRTDS provide quantitative support of cause and effect mechanisms of nutrient impacts on potentially adverse environmental conditions as they relate to nutrient-related source controls upstream.

3.3.2 Effects of biological invasions

Invasion of the upper SFE by the Asian clam *Potamocorbula amurensis* in 1986 caused severe changes in phytoplankton abundance and species composition. Reduction in phytoplankton biomass has altered trophic networks in the Bay and is considered a primary mechanism in the decline of the protected delta smelt (*Hypomesus transpacificus*) and other important fisheries.^{52,53} Changes in the physical environment have also occurred with the most notable invasion effect being increased water clarity following a reduction of phytoplankton by biofiltration.⁵³ The clams are halophilic such that drought years are generally correlated with an increase in biomass and further upstream invasion of the species.^{24,54} We hypothesized that WRTDS models applied to water quality observations in the upper estuary would show 1) a decline in annual, flow-normalized chlorophyll concentrations over time coincident with an increase in abundance of invaders, and 2) variation in the chlorophyll/clam relationship through indirect or direct controls of flow. The application of WRTDS to water quality

observations at station D7 in Suisun Bay and comparison with clam abundance and biomass data (see Ref 34) provides an approach to assess the competing effects of climate variability, hydrology, and ecology on ambient conditions.

Results from WRTDS demonstrated complex relationships between clam abundance and chlorophyll concentrations, which were further affected by flow changes over time (Figure 5). Invasion in the 1980s showed a clear displacement of the native *Corbicula fluminea* with establishment of *P. amurensis* (Figure 5a), where biomass of the latter was negatively associated with flow from the Sacramento river (Figure 5b). The increase in clam abundance was associated with a notable decrease in annually-averaged chl-*a* from WRTDS results (Figure 5c). A seasonal shift in the flow-normalized results was also observed such that chl-*a* concentrations were generally highest in July prior to invasion, whereas a spring maximum in April was more common in recent years (Figure 5d). The relationship of chl-*a* with clam biomass was significant (Figure 5e) with lower chl-*a* associated with higher biomass. The chl-*a*/flow relationship changed over time such that increasing flow (decreasing salinity) showed a slight increase in chl-*a* followed by a decrease early in the time series (Figure 5f), whereas overall chl-*a* was lower but a positive association with flow (negative with salinity) was observed later in the time series.

A general conclusion is that clam grazing reduced chl-*a* concentration throughout the period of record, whereas the effect of flow as a top-down or bottom-up control on both was more dynamic. The relationship between flow and chl-*a* earlier in the time period suggested a dilution effect at high flow and peak chl-*a* at moderate flows. In the absence of benthic grazing prior to invasion, this dynamic suggests that chl-*a* production may be limited at low flow as less nutrients are exported from the Delta, stimulated as flow increases, and reduced at high flow as either nutrients or phytoplankton biomass are exported to the larger bay. Following clam invasion later in the time series, chl-*a* concentrations were reduced by grazing but showed a positive and monotonic relationship with increasing flow. The increase in clam abundance was concurrent with decline in chl-*a* concentration, although variation in

abundance between years was also observed (5a). For example, clam abundance was reduced during high flow years in the late 1990s, 2006, and 2011 (Figure S1). In the same years, WRTDS predictions for chl-*a* were higher than the flow-normalized component (Figure 5c), which further suggests a link between increased flow and phytoplankton production. As such, chl-*a* production in early years is directly related to flow, whereas the relationship with flow in later years is indirect as increased flow reduces clam abundance and releases phytoplankton from benthic grazing pressure. These relationships have been suggested by others,^{27,54,55} although the precise mechanism demonstrated by WRTDS provides a quantitative description of factors that drive water quality in the Delta.

As demonstrated by both case studies and the overall trends across all stations, water quality dynamics in the Delta are complex and driven by multiple factors that change through space and time. At a minimum, WRTDS provides a description of change by focusing on high-level forcing factors that explicitly account for annual, seasonal, and flow effects on trend interpretations. We have demonstrated the potential for imprecise or inaccurate conclusions of trend tests that focus solely on observed data and emphasize that flow-normalized trends have more power to quantify change. Combined with additional data, WRTDS results can support hypotheses that lead to a more comprehensive understanding of ecosystem dynamics. Still, additional sources of variability must be considered as explicit factors that influence observed trends and exploration of alternative time series analysis methods to address a wider range of questions should be the focus of further analyses. Additional factors to consider include the effects of large-scale climatic patterns, more detailed hydrologic descriptions, and additional ecological components that affect trophic interactions. Statistical interpretations of multiple factors can provide a basis for quantitative links between nutrient loads and adverse effects on ecosystem conditions, including the identification of thresholds for the protection and restoration of water quality.

References

- (1) O'Neill, R. V.; Johnson, A. R.; King, A. W. A hierarchical framework for the analysis of scale. *Landscape Ecology* **1989**, *3*, 193–205.
- (2) Levin, S. A. The problem of pattern and scale in ecology. *Ecology* **1992**, *73*, 1943–1967.
- (3) Bhangu, I.; Whitfield, P. H. Seasonal and long-term variations in water quality of the Skeena River at Usk, British Columbia. *Water Research* **1997**, *31*, 2187–2194.
- (4) Champely, S.; Doledec, S. How to separate long-term trends from periodic variation in water quality monitoring. *Water Research* **1997**, *31*, 2849–2857.
- (5) Chang, H. Spatial analysis of water quality trends in the Han River basin, South Korea. *Water Research* **2008**, *42*, 3285–3304.
- (6) Halliday, S. J.; Wade, A. J.; Skeffington, R. A.; Neal, C.; Reynolds, B.; Rowland, P.; Neal, M.; Norris, D. An analysis of long-term trends, seasonality and short-term dynamics in water quality data from Plynlimon, Wales. *Science of the Total Environment* **2012**, *434*, 186–200.
- (7) Cloern, J. E. Phytoplankton bloom dynamics in coastal ecosystems: A review with some general lessons from sustained investigation of San Francisco Bay, California. *Review of Geophysics* **1996**, *34*, 127–168.
- (8) Cloern, J. E.; Jassby, A. D. Patterns and scales of phytoplankton variability in estuarine-coastal ecosystems. *Estuaries and Coasts* **2010**, *33*, 230–241.
- (9) Sakamoto, M.; Tanaka, T. Phosphorus dynamics associated with phytoplankton blooms in eutrophic Mikawa Bay, Japan. *Marine Biology* **1989**, *101*, 265–271.
- (10) Schultz, P.; Urban, N. R. Effects of bacterial dynamics on organic matter decomposition and nutrient release from sediments: A modeling study. *Ecological Modelling* **2008**, *210*, 1–14.
- (11) Harding, L. W.; Gallegos, C. L.; Perry, E. S.; Miller, W. D.; Adolf, J. E.; Mallonee, M. E.; Paerl, H. W. Long-term trends of nutrients and phytoplankton in Chesapeake Bay. *Estuaries and Coasts* **2016**, *39*, 664–681.
- (12) Hirsch, R. M.; Alexander, R. B.; Smith, R. A. Selection of methods for the detection and estimation of trends in water quality. *Water Resources Research* **1991**, *27*, 803–813.
- (13) Esterby, S. R. Review of methods for the detection and estimation of trends with emphasis on water quality applications. *Hydrological Processes* **1996**, *10*, 127–149.
- (14) Bowes, M. J.; Smith, J. T.; Neal, C. The value of high resolution nutrient monitoring: a case study of the River Frome, Dorset, UK. *Journal of Hydrology* **2009**, *378*, 82–96.

- (15) Hirsch, R. M.; Moyer, D. L.; Archfield, S. A. Weighted regressions on time, discharge, and season (WRTDS), with an application to Chesapeake Bay river inputs. *Journal of the American Water Resources Association* **2010**, *46*, 857–880.
- (16) Sprague, L. A.; Hirsch, R. M.; Aulenbach, B. T. Nitrate in the Mississippi River and its tributaries, 1980 to 2008: Are we making progress? *Environmental Science and Technology* **2011**, *45*, 7209–7216.
- (17) Medalie, L.; Hirsch, R. M.; Archfield, S. A. Use of flow-normalization to evaluate nutrient concentration and flux changes in Lake Champlain tributaries, 1990–2009. *Journal of Great Lakes Research* **2012**, *38*, 58–67.
- (18) Hirsch, R. M.; De Cicco, L. *User guide to Exploration and Graphics for RivEr Trends (EGRET) and dataRetrieval: R packages for hydrologic data*; 2014; p 94, <http://pubs.usgs.gov/tm/04/a10/>.
- (19) Zhang, Q.; Harman, C. J.; Ball, W. P. An improved method for interpretation of riverine concentration-discharge relationships indicates long-term shifts in reservoir sediment trapping. *Geophysical Research Letters* **2016**, *43*, 215–224.
- (20) Beck, M. W.; Hagy III, J. D. Adaptation of a weighted regression approach to evaluate water quality trends in an estuary. *Environmental Modelling and Assessment* **2015**, *20*, 637–655.
- (21) Beck, M. W.; Murphy, R. R. Numerical and qualitative contrasts of two statistical models for water quality change in tidal waters. *Journal of the American Water Resources Association* **In press**,
- (22) Beck, M. W.; Hagy III, J. D.; Murrell, M. C. Improving estimates of ecosystem metabolism by reducing effects of tidal advection on dissolved oxygen time series. *Limnology and Oceanography: Methods* **2015**, *13*, 731–745.
- (23) Cloern, J. E. In *Ecosystems of California: A Source Book*; Mooney, H., Zavaleta, E., Eds.; University of California Press: California, 2015; pp 359–387.
- (24) Cloern, J. E.; Jassby, A. D. Drivers of change in estuarine-coastal ecosystems: Discoveries from four decades of study in San Francisco Bay. *Reviews of Geophysics* **2012**, *50*, 1–33.
- (25) Jassby, A. D.; Cloern, J. E. Organic matter sources and rehabilitations of the Sacramento-San Joaquin Delta (California, USA. **2000**,
- (26) Jassby, A. D.; Cloern, J. E.; Cole, B. E. Annual primary production: Patterns and mechanisms of change in a nutrient-rich tidal ecosystem. *Limnology and Oceanography* **2002**, *47*, 698–712.
- (27) Jassby, A. D. Phytoplankton in the Upper San Francisco Estuary: Recent biomass trends, their causes, and their trophic significance. *San Francisco Estuary and Watershed Science* **2008**, *6*, 1–24.

- (28) Jabusch, T.; Bresnahan, P.; Trowbridge, P.; Novick, E.; Wong, A.; Salomon, M.; Senn, D. *Summary and evaluation of Delta subregions for nutrient monitoring and assessment*; 2016.
- (29) Novick, E.; Holleman, R.; Jabusch, T.; Sun, J.; Trowbridge, P.; Senn, D.; Guerin, M.; Kendall, C.; Young, M.; Peek, S. *Characterizing and quantifying nutrient sources, sinks and transformations in the Delta: synthesis, modeling, and recommendations for monitoring*; 2015.
- (30) Cloern, J. E.; Jassby, A. D.; Thompson, J. K.; Hieb, K. A. A cold phase of the East Pacific triggers new phytoplankton blooms in San Francisco Bay. *Proceedings of the National Academy of Sciences of the United States of America* **2007**, *104*, 18561–18565.
- (31) Kemp, W. M. et al. Eutrophication of Chesapeake Bay: historical trends and ecological interactions. *Marine Ecology Progress Series* **2005**, *303*, 1–29.
- (32) Kimmerer, W. J.; Parker, A. E.; Lidstrom, U. E.; Carpenter, E. J. Short-term and interannual variability in primary production in the low-salinity zone of the San Francisco Estuary. *Estuaries and Coasts* **2012**, *35*, 913–929.
- (33) Thompson, J. K.; Koseff, J. R.; Monismith, S. G.; Lucas, L. V. Shallow water processes govern system-wide phytoplankton bloom dynamics: A field study. *Journal of Marine Systems* **2008**, *74*, 153–166.
- (34) Crauder, J. S.; Thompson, J. K.; Parchaso, F.; Anduaga, R. I.; Pearson, S. A.; Gehrts, K.; Fuller, H.; Wells, E. *Bivalve effects on the food web supporting delta smelt - A long-term study of bivalve recruitment, biomass, and grazing rate patterns with varying freshwater outflow*; 2016.
- (35) Sutula, M.; Kudela, R.; III, J. D. H.; Jr., L. W. H.; Senn, D.; Cloern, J. E.; Bricker, S.; Berg, G. M.; Beck, M. W. Novel analyses of long-term data provide a scientific basis for chlorophyll-a thresholds in San Francisco Bay. *Estuarine, Coastal and Shelf Science* **in review**,
- (36) Lehman, P. W.; Boyer, G.; Hall, C.; Waller, S.; Gehrts, K. Distribution and toxicity of a new colonial *Microcystis aeruginosa* bloom in the San Francisco Bay Estuary, California. *Hydrobiologia* **2005**, *541*, 87–99.
- (37) Lehman, P. W.; Teh, S. J.; Boyer, G. L.; Nobriga, M. L.; Bass, E.; Hogle, C. Initial impacts of *Microcystis aeruginosa* blooms on the aquatic food web in the San Francisco Estuary. *Hydrobiologia* **2010**, *637*, 229–248.
- (38) Cohen, A. N.; Carlton, J. T. Accelerating invasion rate in a highly invaded estuary. *Science* **1998**, *279*, 555–558.
- (39) Enright, C.; Culberson, S. D. Salinity trends, variability, and control in the northern reach of the San Francisco Estuary. *San Francisco Estuary & Watershed Science* **2009**, *7*, 1–28.

- (40) Dugdale, R. C.; Wilkerson, F. P.; Hogue, V. E.; Marchi, A. The role of ammonium and nitrate in spring bloom development in San Francisco Bay. *Estuarine, Coastal, and Shelf Science* **2007**, *73*, 17–29.
- (41) Parker, A. E.; Hogue, V. E.; Wilkerson, F. P.; Dugdale, R. C. The effect of inorganic nitrogen speciation on primary production in the San Francisco Estuary. *Estuarine, Coastal, and Shelf Science* **2012**, *104*, 91–101.
- (42) Glibert, P. M.; Dugdale, R. C.; Wilkerson, F.; Parker, A. E.; Alexander, J.; Antell, E.; Blaser, S.; Johnson, A.; Lee, J.; Lee, T.; Murasko, S.; Strong, S. Major - but rare - spring blooms in San Francisco Bay Delta, California, a result of long-term drought, increased residence time, and altered nutrient loads and forms. *Journal of Experimental Marine Biology and Ecology* **2014**, *460*, 8–18.
- (43) IEP, IEP Bay-Delta Monitoring and Analysis Section, Discrete Water Quality Metadata. 2013; <http://water.ca.gov/bdma/meta/discrete.cfm>.
- (44) IEP, Dayflow: An estimate of daily average Delta outflow. Interagency Ecological Program for the San Francisco Estuary. 2016; <http://www.water.ca.gov/dayflow/>.
- (45) Moyer, D. L.; Hirsch, R. M.; Hyer, K. E. *Comparison of two regression-based approaches for determining nutrient and sediment fluxes and trends in the Chesapeake Bay Watershed*; 2012; p 118.
- (46) Tobin, J. Estimation of relationships for limited dependent variables. *Econometrica* **1958**, *26*, 24–36.
- (47) Beck, M. W. WRTDStidal: Weighted Regression for Water Quality Evaluation in Tidal Waters. 2016; R package version 1.0.2.
- (48) RDCT (R Development Core Team), R: A language and environment for statistical computing, v3.3.1. R Foundation for Statistical Computing, Vienna, Austria. 2016; <http://www.R-project.org>.
- (49) Hirsch, R. M.; Slack, J. R.; Smith, R. A. Techniques of trend analysis for monthly water quality data. *Water Resources Research* **1982**, *18*, 107–121.
- (50) Millard, S. P. *EnvStats: An R Package for Environmental Statistics*; Springer: New York, 2013.
- (51) Cornwell, J. C.; Glibert, P. M.; Owens, M. S. Nutrient fluxes from sediments in the San Francisco Bay Delta. *Estuaries and Coasts* **2014**, *37*, 1120–1133.
- (52) Feyrer, F.; Herbold, B.; Matern, S. A.; Moyle, P. B. Dietary shifts in a stressed fish assemblage: Consequences of a bivalve invasion in the San Francisco Estuary. *Environmental Biology of Fishes* **2003**, *67*, 277–288.

- (53) Mac Nally, R.; Thompson, J. R.; Kimmerer, W. J.; Feyrer, F.; Newman, K. B.; Sih, A.; Bennett, W. A.; Brown, L.; Fleishman, E.; Culberson, S. D.; Castillo, G. Analysis of pelagic species decline in the upper San Francisco Estuary using multivariate autoregressive modeling (MAR). *Ecological Applications* **2010**, *20*, 1417–1430.
- (54) Parchaso, F.; Thompson, J. K. Influence of hydrologic processes on reproduction of the introduced bivalve *Potamocorbula amurensis* in northern San Francisco Bay, California. *Pacific Science* **2002**, *56*, 329–345.
- (55) Alpine, A. E.; Cloern, J. E. Trophic interactions and direct physical effects control phytoplankton biomass and production in an estuary. *Limnology and Oceanography* **1992**, *37*, 946–955.

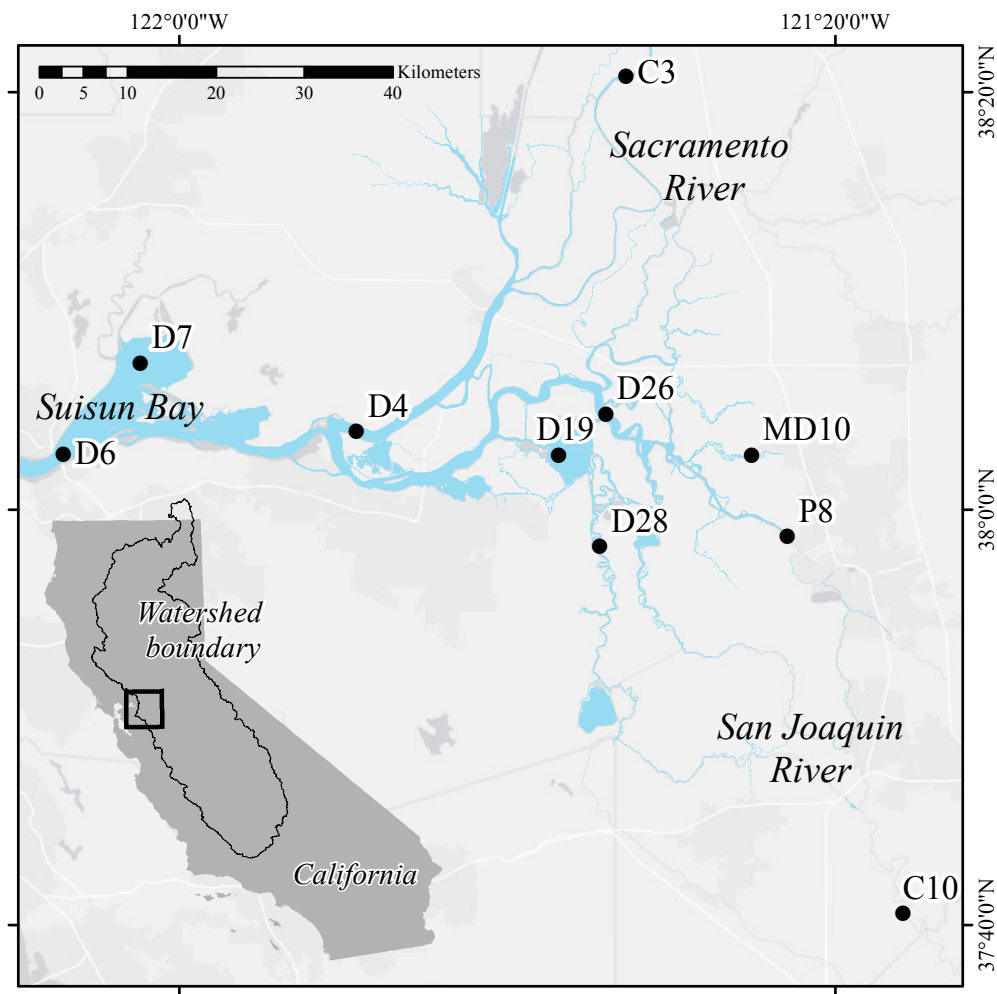


Figure 1: The San Francisco Estuary Delta and monitoring stations used for analysis. The Delta drains the combined watersheds of the Sacramento and San Joaquin rivers (bottom left). All data were obtained from the Interagency Ecological Program website (<http://water.ca.gov/bdma/meta/Discrete/data.cfm>).⁴³

{fig:delt_m

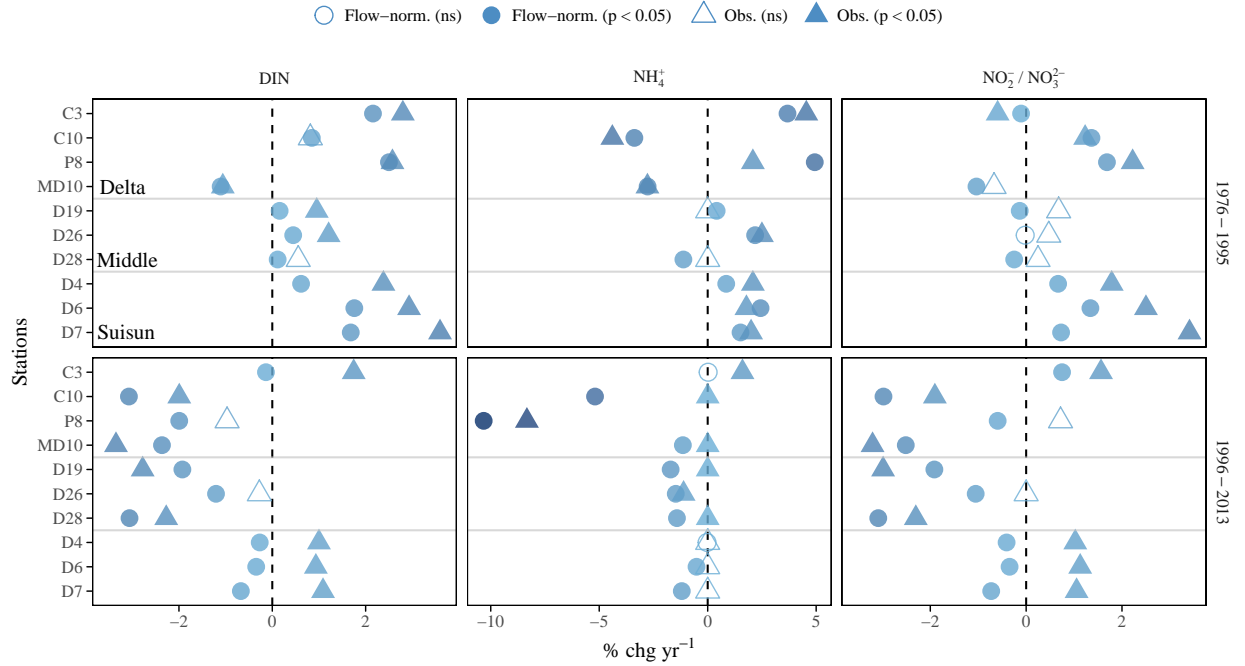


Figure 2: Results from seasonal Kendall tests on observed data (triangles) and flow-normalized predictions (circles) from WRTDS for nitrogen analytes. Results are shown as the percent change per year as the estimated Theil-Sen slope divided by the median for a given aggregation period (significance evaluated at $\alpha = 0.05$, based on τ). Trends are shown separately for different annual groupings. See Figures S2 and S3 for seasonal groupings.

{fig:trndco

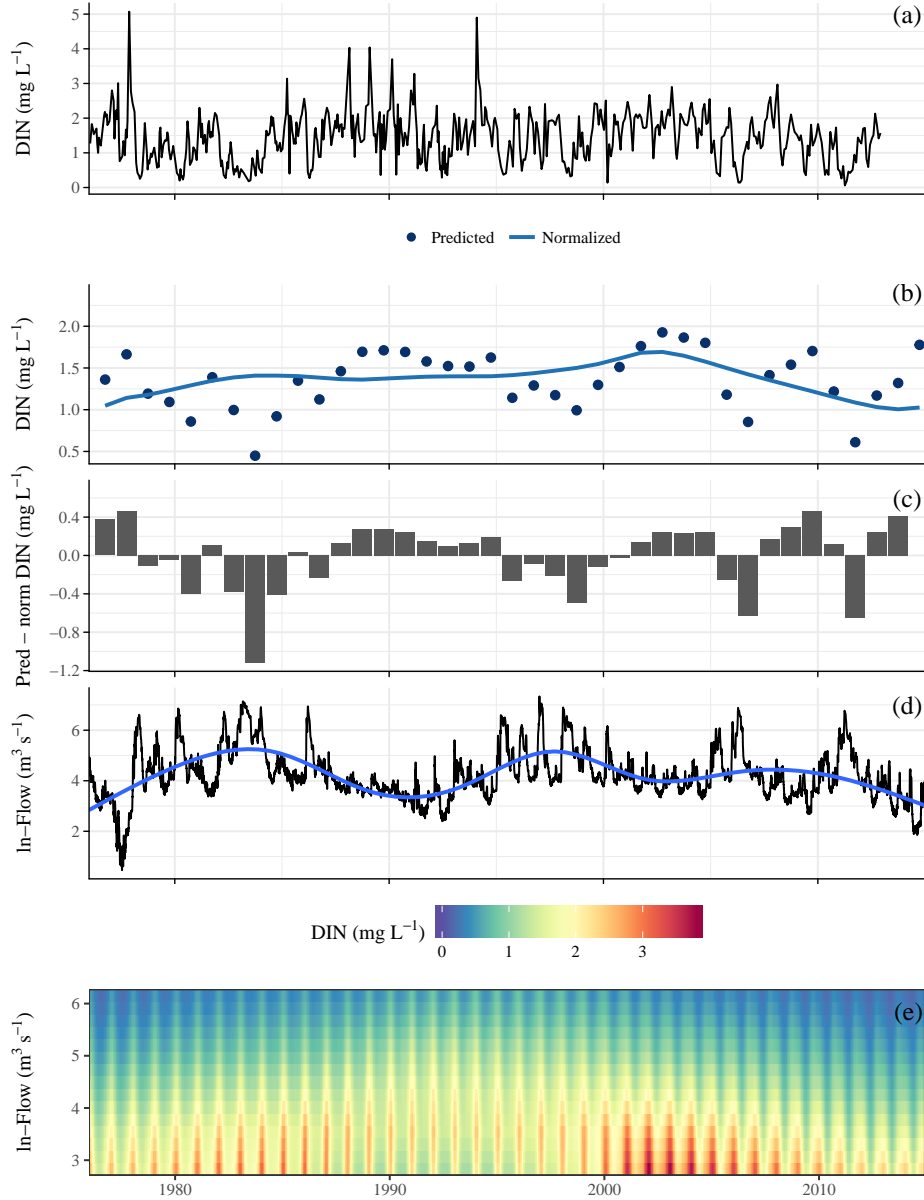


Figure 3: Time series of DIN and flow at station C10. Subfigure (a) shows the observed DIN time series and subfigure (b) shows the annual (water year starting in October) predictions from WRTDS for the conditional mean response. The points in subfigure (b) are predictions of observed DIN and the lines are flow-normalized predictions. Subfigure (c) shows the difference between the model predictions and flow-normalized predictions. Subfigure (d) shows the flow time series of the San Joaquin River with a locally-estimated (loess) smooth to emphasize the long-term trend. Subfigure (e) shows the modelled relationships between DIN, flow (5th and 95th percentiles), and time.

{fig:dinc10

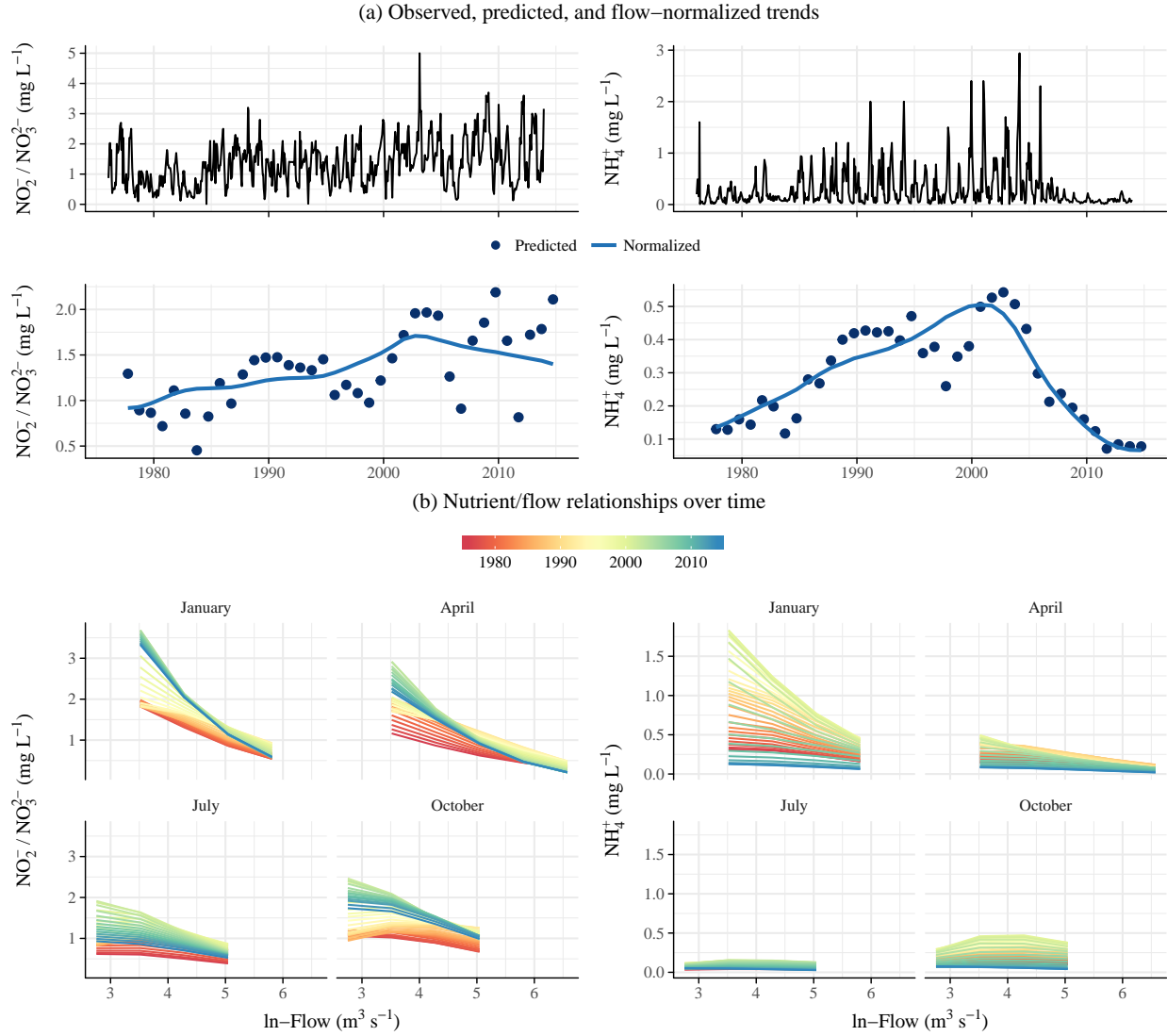


Figure 4: Nitrogen trends at P8 as (a, top) observed, (a, bottom) predicted and flow-normalized estimates from WRTDS, and (b) relationships with flow over time from WRTDS. Nitrite/nitrate trends are on the left and ammonium trends are on the right. Wastewater treatment plant upgrades at the City of Stockton (San Joaquin County) were completed in 2006 (Figure S4).

{fig:p8trnd

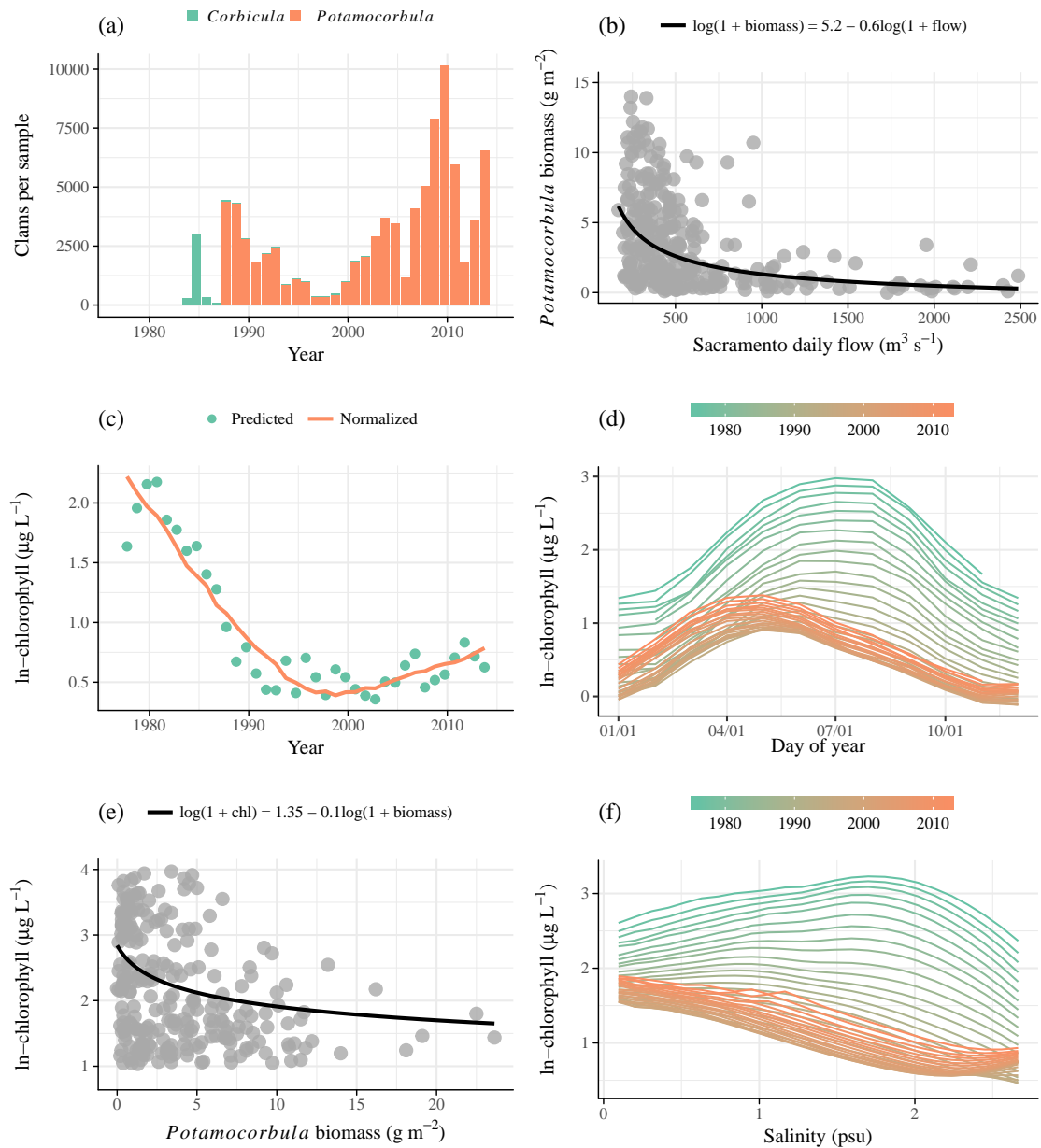


Figure 5: Trends in clam abundance and chl-*a* concentration from 1976 to 2013 at station D7 in Suisun Bay. Invasion by *Potamocorbula amurensis* clams in the late 1980s and displacement of *Corbicula fluminea* was shown by changes in clam density (a, annual means), with biomass linked to salinity (b). A decrease in chl-*a* concentration was also observed by changes in annual (c) and seasonal trends(d) based on WRTDS results. A significant ($p < 0.001$) relationship between clam biomass and chl-*a* concentration is shown in subfigure (e). Flow relationships with chl-*a* concentration shown by WRTDS have also changed over time (f, observations from June).

{fig:clmchl}

Table 1: Summaries of flow-normalized trends in nitrite/nitrate and ammonium (mg L^{-1}) concentrations before and after WWTP upgrades upstream of station P8. Upgrades were completed in 2006 at the City of Stockton WWTP (San Joaquin County, Figure S4). Summaries are medians and percent change per year in parentheses (increasing in bold-italic). Changes and significance estimates are based on seasonal Kendall tests of flow-normalized results within each time period. Increasing values are in bold-italics. Months for each season are Spring: MAM, Summer: JJA, Fall: SON, Winter: DJF.

{tab:p8chg}

Period	$\text{NO}_2^-/\text{NO}_3^-$		NH_4^+	
	Median	% change	Median	% change
Annual				
1976-2006	1.3	<i>2**</i>	0.2	<i>2.8**</i>
2007-2013	1.4	-1.9**	0.1	-16.6**
Seasonal, pre				
Spring	1.2	<i>1.6**</i>	0.2	<i>1.4**</i>
Summer	1	<i>2.4**</i>	0.1	<i>3.3**</i>
Fall	1.3	<i>2.2**</i>	0.2	<i>4.9**</i>
Winter	1.5	<i>2.1**</i>	0.7	<i>4.8**</i>
Seasonal, post				
Spring	1.3	-1.6**	0.1	-16.2**
Summer	0.9	-4.3**	0.1	-15.7**
Fall	1.5	-1.7**	0.1	-19.3**
Winter	2.2	-0.8**	0.2	-26.7**

* $p < 0.05$; ** $p < 0.005$

606 **Supporting Information Available**

607 The following files are available free of charge.

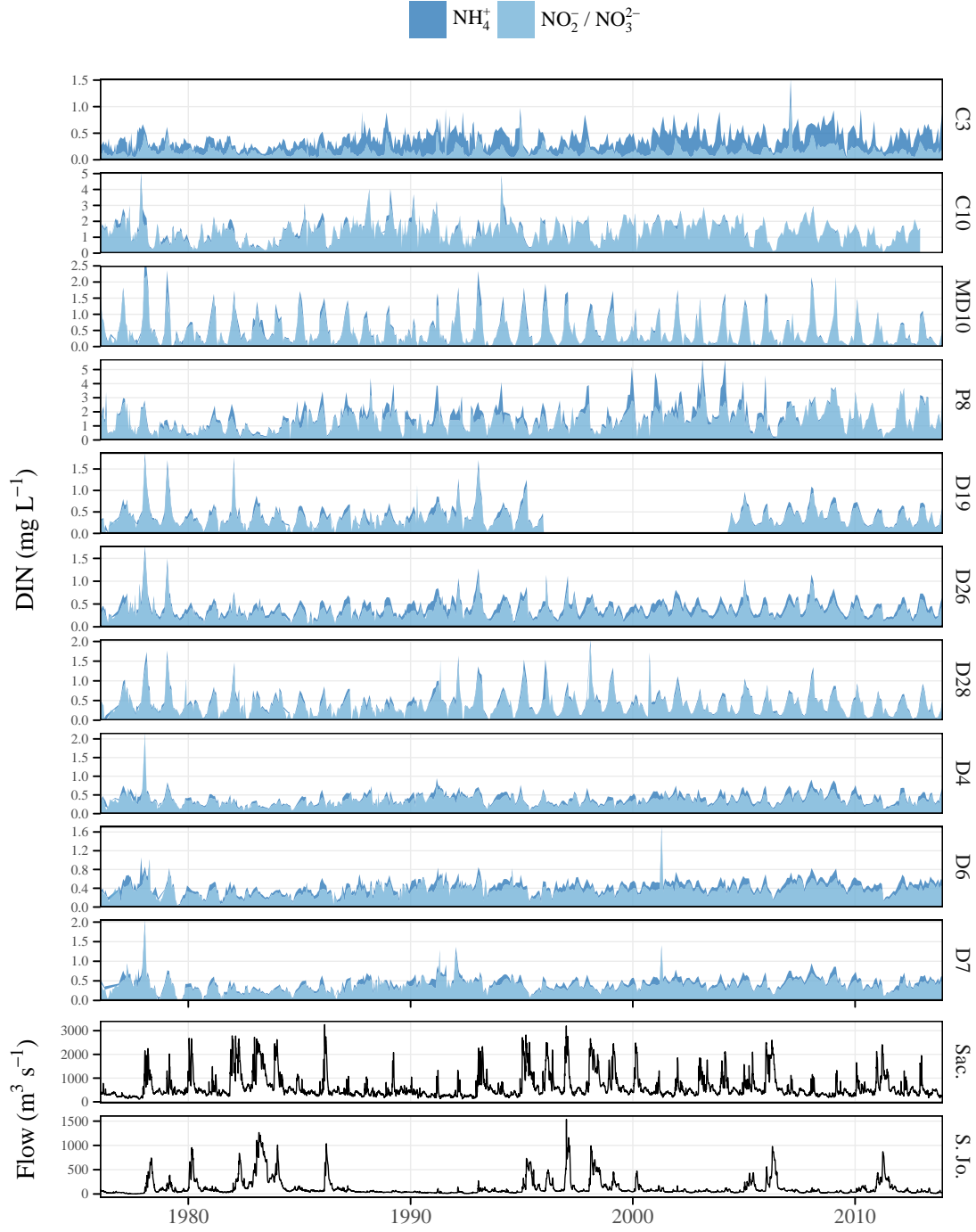


Figure S1: Observed DIN ($\text{NH}_4^+ + \text{NO}_2^- / \text{NO}_3^{2-}$) from ten stations in the upper SFE Delta and flow from the Sacramento and San Joaquin rivers. Data were collected monthly and evaluated with WRTDS models using daily flow estimates from 1976 to 2013. Note different y-axis scales. See Figure 1 for station locations.

{fig:obsdat

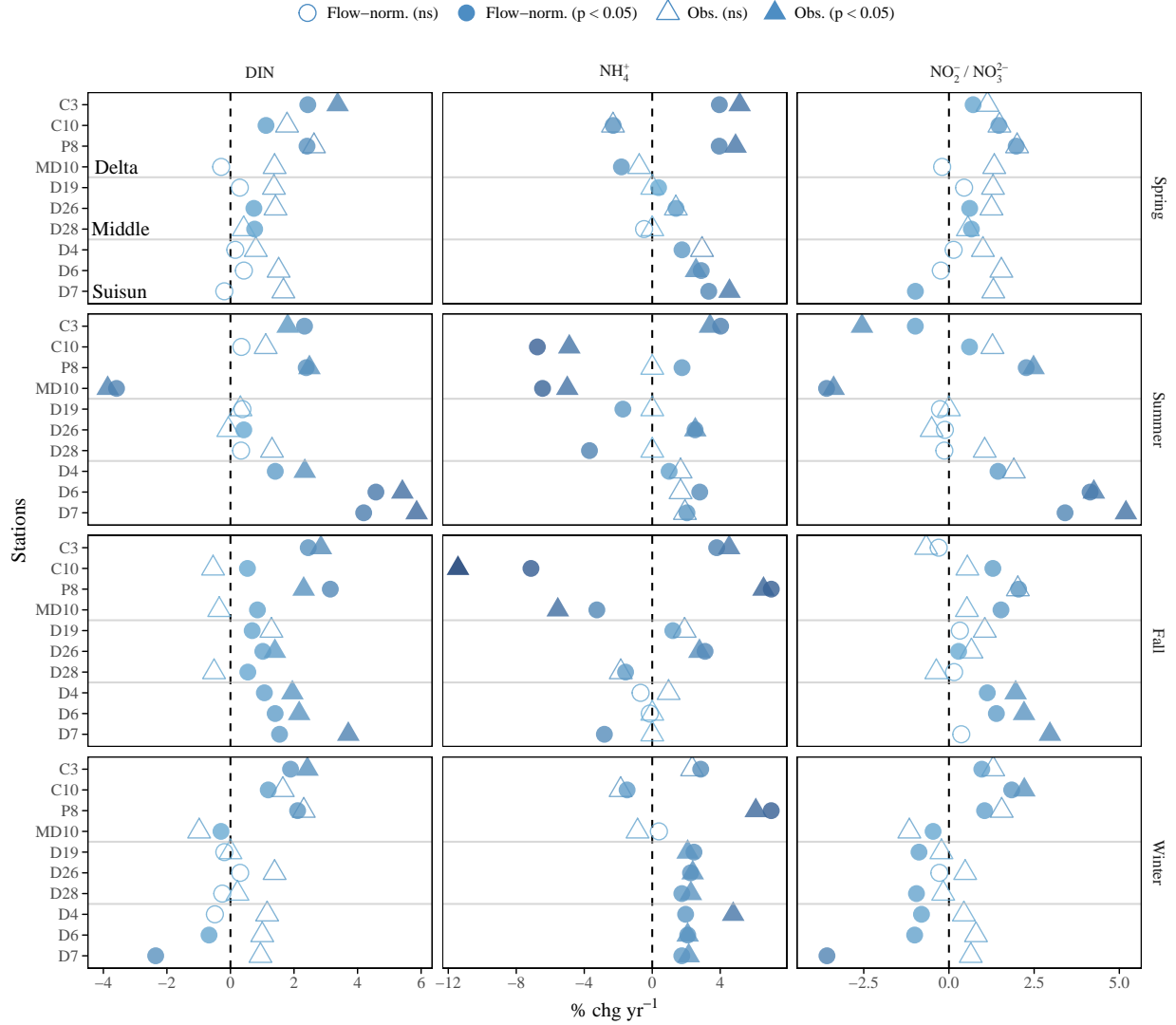


Figure S2: Results from seasonal Kendall tests on observed data (triangles) and flow-normalized predictions (circles) from WRTDS for nitrogen analytes. Results are shown as the percent change per year as the estimated Theil-Sen slope divided by the median for a given aggregation period (significance evaluated at $\alpha = 0.05$, based on τ). Trends are shown separately for different seasonal groupings from 1976-1995. Months for each season are Spring: MAM, Summer: JJA, Fall: SON, Winter: DJF. See Figure 2 for annual comparisons.

{fig:trndcc}

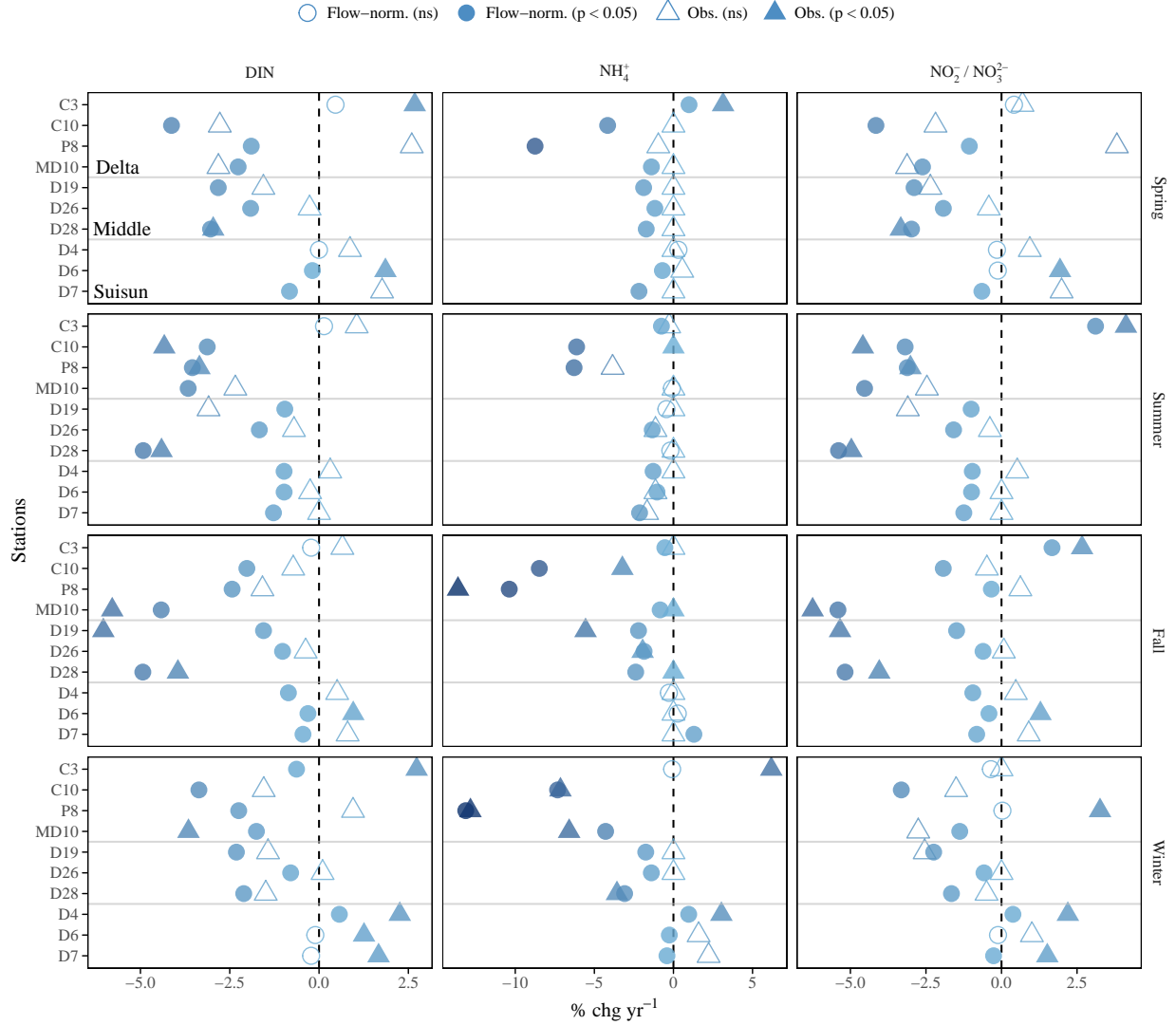


Figure S3: Results from seasonal Kendall tests on observed data (triangles) and flow-normalized predictions (circles) from WRTDS for nitrogen analytes. Results are shown as the percent change per year as the estimated Theil-Sen slope divided by the median for a given aggregation period (significance evaluated at $\alpha = 0.05$, based on τ). Trends are shown separately for different seasonal groupings from 1996-2013. Months for each season are Spring: MAM, Summer: JJA, Fall: SON, Winter: DJF. See Figure 2 for annual comparisons.

{fig:trndcc}

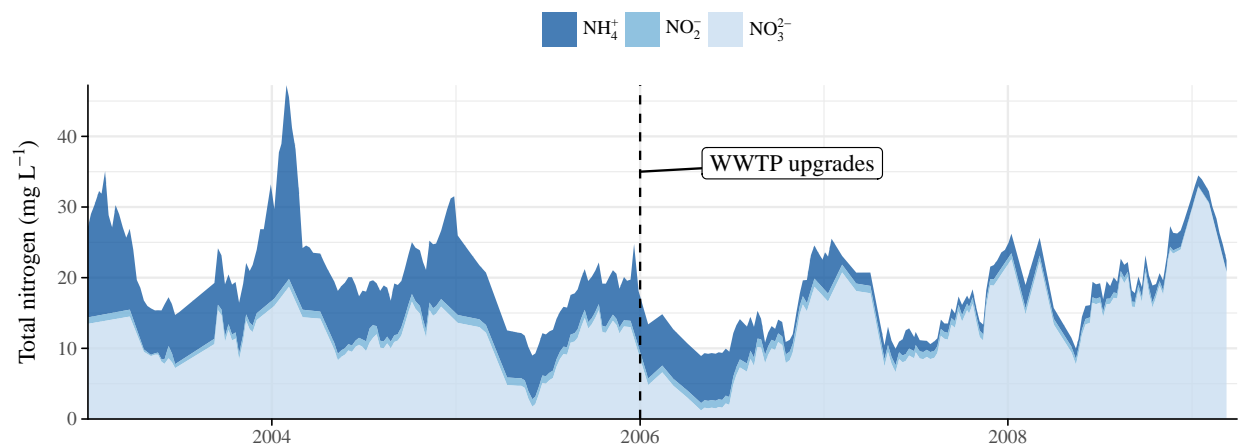


Figure S4: Nitrogen concentration measurements (mg L^{-1}) from the City of Stockton Wastewater Treatment Plant, San Joaquin County. Wastewater discharge requirements were implemented in 2006 for nitrification/denitrification and tertiary filtration to convert ammonium to nitrate.

{fig:stock}

Table S1: Summaries of flow-normalized trends in nitrogen analytes for all stations and annual aggregations. Summaries are medians (mg L⁻¹) and percent change per year in parentheses (increasing in bold-italic). Changes and significance estimates are based on seasonal Kendall tests of flow-normalized results within each time period.

{tab:trnds}

Analyte/Station	Annual	
	1976-1995	1996-2013
DIN		
C10	1.3 (<i>0.8</i>)**	1.4 (-3.1)**
C3	0.3 (<i>2.2</i>)**	0.5 (-0.1)**
D19	0.4 (<i>0.2</i>)**	0.4 (-1.9)**
D26	0.4 (<i>0.4</i>)**	0.5 (-1.2)**
D28	0.4 (<i>0.1</i>)**	0.4 (-3.1)**
D4	0.3 (<i>0.6</i>)**	0.4 (-0.3)**
D6	0.4 (<i>1.8</i>)**	0.5 (-0.3)**
D7	0.4 (<i>1.7</i>)**	0.5 (-0.7)**
MD10	0.4 (-1.1)**	0.3 (-2.4)**
P8	1.3 (<i>2.5</i>)**	1.7 (-2)**
NH₄⁺		
C10	0.1 (-3.4)**	0 (-5.2)**
C3	0.2 (<i>3.7</i>)**	0.3 (<i>0</i>)
D19	0 (<i>0.4</i>)**	0 (-1.7)**
D26	0.1 (<i>2.2</i>)**	0.1 (-1.5)**
D28	0 (-1.1)**	0 (-1.4)**
D4	0 (<i>0.9</i>)**	0.1 (<i>0</i>)
D6	0.1 (<i>2.4</i>)**	0.1 (-0.5)**
D7	0.1 (<i>1.5</i>)**	0.1 (-1.2)**
MD10	0.1 (-2.8)**	0 (-1.1)**
P8	0.2 (<i>4.9</i>)**	0.1 (-10.3)**
NO₂⁻/NO₃²⁻		
C10	1.2 (<i>1.4</i>)**	1.4 (-3)**
C3	0.1 (-0.1)**	0.2 (<i>0.7</i>)**
D19	0.4 (-0.1)**	0.4 (-1.9)**
D26	0.3 (<i>0</i>)	0.4 (-1.1)**
D28	0.4 (-0.2)**	0.4 (-3.1)**
D4	0.3 (<i>0.7</i>)**	0.3 (-0.4)**
D6	0.3 (<i>1.3</i>)**	0.4 (-0.3)**
D7	0.4 (<i>0.7</i>)**	0.4 (-0.7)**
MD10	0.4 (-1)**	0.3 (-2.5)**
P8	1.2 (<i>1.7</i>)**	1.5 (-0.6)**

* $p < 0.05$; ** $p < 0.005$

Table S2: Summaries of flow-normalized trends in nitrogen analytes for all stations and seasonal aggregations from 1976-1995. Summaries are medians (mg L⁻¹) and percent change per year in parentheses (increasing in bold-italic). Changes and significance estimates are based on seasonal Kendall tests of flow-normalized results within each time period. Months for each season are Spring: MAM, Summer: JJA, Fall: SON, Winter: DJF.

{tab:trndsb

Analyte/Station	Seasonal, 1976-1995			
	Spring	Summer	Fall	Winter
DIN				
C10	1.2 (<i>1.1</i>)**	1.2 (<i>0.3</i>)	1.3 (<i>0.5</i>)**	1.7 (<i>1.2</i>)**
C3	0.3 (<i>2.4</i>)**	0.3 (<i>2.3</i>)**	0.4 (<i>2.4</i>)**	0.4 (<i>1.9</i>)**
D19	0.5 (<i>0.3</i>)	0.2 (<i>0.4</i>)	0.3 (<i>0.7</i>)**	0.7 (-0.2)
D26	0.4 (<i>0.7</i>)**	0.3 (<i>0.4</i>)*	0.4 (<i>1</i>)**	0.6 (<i>0.3</i>)
D28	0.5 (<i>0.8</i>)*	0.2 (<i>0.3</i>)	0.3 (<i>0.5</i>)*	0.8 (-0.3)
D4	0.4 (<i>0.2</i>)	0.3 (<i>1.4</i>)**	0.3 (<i>1.1</i>)**	0.5 (-0.5)
D6	0.4 (<i>0.4</i>)	0.3 (<i>4.6</i>)**	0.4 (<i>1.4</i>)**	0.5 (-0.7)*
D7	0.4 (-0.2)	0.3 (<i>4.2</i>)**	0.4 (<i>1.5</i>)**	0.6 (-2.4)**
MD10	0.6 (-0.3)	0.2 (-3.6)**	0.3 (<i>0.8</i>)**	1.3 (-0.3)*
P8	1.3 (<i>2.4</i>)**	0.9 (<i>2.4</i>)**	1.3 (<i>3.1</i>)**	1.9 (<i>2.1</i>)**
NH₄⁺				
C10	0.1 (-2.3)**	0 (-6.8)**	0.1 (-7.1)**	0.3 (-1.5)**
C3	0.2 (<i>3.9</i>)**	0.2 (<i>4</i>)**	0.3 (<i>3.8</i>)**	0.2 (<i>2.9</i>)**
D19	0.1 (<i>0.4</i>)*	0 (-1.7)**	0 (<i>1.2</i>)**	0.1 (<i>2.5</i>)**
D26	0.1 (<i>1.4</i>)**	0.1 (<i>2.5</i>)**	0.1 (<i>3.1</i>)**	0.1 (<i>2.3</i>)**
D28	0.1 (-0.5)	0 (-3.7)**	0 (-1.6)**	0.1 (<i>1.7</i>)**
D4	0.1 (<i>1.7</i>)**	0 (<i>1</i>)**	0 (-0.7)	0.1 (<i>2</i>)**
D6	0.1 (<i>2.9</i>)**	0.1 (<i>2.8</i>)**	0.1 (-0.1)	0.1 (<i>2.1</i>)**
D7	0.1 (<i>3.3</i>)**	0 (<i>2</i>)**	0.1 (-2.8)**	0.1 (<i>1.7</i>)**
MD10	0.1 (-1.8)**	0 (-6.5)**	0 (-3.3)**	0.2 (<i>0.4</i>)
P8	0.2 (<i>3.9</i>)**	0.1 (<i>1.8</i>)**	0.2 (<i>7</i>)**	0.6 (<i>7</i>)**
NO₂⁻/NO₃²⁻				
C10	1.1 (<i>1.5</i>)**	1.2 (<i>0.6</i>)**	1.2 (<i>1.3</i>)**	1.5 (<i>1.8</i>)**
C3	0.2 (<i>0.7</i>)**	0.1 (-1)**	0.1 (-0.3)	0.2 (<i>1</i>)**
D19	0.4 (<i>0.4</i>)	0.2 (-0.3)	0.3 (<i>0.3</i>)	0.6 (-0.9)*
D26	0.4 (<i>0.6</i>)*	0.2 (-0.1)	0.3 (<i>0.3</i>)*	0.5 (-0.3)
D28	0.5 (<i>0.7</i>)*	0.2 (-0.1)	0.3 (<i>0.2</i>)	0.7 (-1)**
D4	0.3 (<i>0.1</i>)	0.3 (<i>1.4</i>)**	0.3 (<i>1.1</i>)**	0.4 (-0.8)*
D6	0.4 (-0.2)	0.3 (<i>4.1</i>)**	0.3 (<i>1.4</i>)**	0.4 (-1)**
D7	0.4 (-1)*	0.3 (<i>3.4</i>)**	0.4 (<i>0.4</i>)	0.4 (-3.6)**
MD10	0.5 (-0.2)	0.2 (-3.6)**	0.2 (<i>1.5</i>)**	1.2 (-0.5)*
P8	1.2 (<i>2</i>)**	0.9 (<i>2.3</i>)**	1.1 (<i>2</i>)**	1.4 (<i>1</i>)**

* $p < 0.05$; ** $p < 0.005$

Table S3: Summaries of flow-normalized trends in nitrogen analytes for all stations and seasonal aggregations from 1996-2013. Summaries are medians (mg L⁻¹) and percent change per year in parentheses (increasing in bold-italic). Changes and significance estimates are based on seasonal Kendall tests of flow-normalized results within each time period. Months for each season are Spring: MAM, Summer: JJA, Fall: SON, Winter: DJF.

{tab:trnds}

Analyte/Station	Seasonal, 1996-2013			
	Spring	Summer	Fall	Winter
DIN				
C10	1.1 (-4.1)**	1.3 (-3.1)**	1.6 (-2)**	1.7 (-3.4)**
C3	0.5 (0.5)	0.4 (0.1)	0.6 (-0.2)	0.5 (-0.6)**
D19	0.5 (-2.8)**	0.2 (-1)*	0.3 (-1.6)**	0.7 (-2.3)**
D26	0.5 (-1.9)**	0.3 (-1.7)**	0.4 (-1)**	0.6 (-0.8)**
D28	0.5 (-3)**	0.2 (-4.9)**	0.2 (-4.9)**	0.7 (-2.1)**
D4	0.4 (0)	0.4 (-1)**	0.4 (-0.9)**	0.5 (0.6)**
D6	0.5 (-0.2)*	0.5 (-1)**	0.5 (-0.3)*	0.5 (-0.1)
D7	0.5 (-0.8)**	0.4 (-1.3)**	0.4 (-0.4)**	0.6 (-0.2)
MD10	0.4 (-2.3)**	0.2 (-3.7)**	0.2 (-4.4)**	1 (-1.8)**
P8	1.5 (-1.9)**	1.2 (-3.5)**	1.8 (-2.4)**	2.7 (-2.2)**
NH₄⁺				
C10	0 (-4.2)**	0 (-6.1)**	0 (-8.5)**	0.1 (-7.3)**
C3	0.3 (1)**	0.3 (-0.8)*	0.4 (-0.5)*	0.2 (-0.1)
D19	0 (-1.9)**	0 (-0.4)	0 (-2.2)**	0.1 (-1.8)**
D26	0.1 (-1.2)**	0.1 (-1.3)**	0.1 (-1.9)**	0.1 (-1.4)**
D28	0 (-1.7)**	0 (-0.2)	0 (-2.4)**	0.1 (-3.1)**
D4	0.1 (0.3)	0 (-1.3)**	0.1 (-0.3)	0.1 (1)**
D6	0.1 (-0.7)**	0.1 (-1)**	0.1 (0.3)	0.1 (-0.3)**
D7	0.1 (-2.2)**	0 (-2.1)**	0.1 (1.3)**	0.1 (-0.4)*
MD10	0 (-1.4)*	0 (-0.1)	0 (-0.8)**	0.1 (-4.3)**
P8	0.2 (-8.7)**	0.1 (-6.3)**	0.2 (-10.4)**	0.5 (-13.1)**
NO₂⁻/NO₃²⁻				
C10	1.1 (-4.2)**	1.2 (-3.2)**	1.6 (-1.9)**	1.6 (-3.3)**
C3	0.2 (0.4)	0.1 (3.1)**	0.2 (1.7)**	0.2 (-0.4)
D19	0.4 (-2.9)**	0.2 (-1)*	0.3 (-1.5)**	0.6 (-2.2)**
D26	0.4 (-1.9)**	0.2 (-1.6)**	0.3 (-0.6)*	0.5 (-0.6)**
D28	0.5 (-3)**	0.2 (-5.4)**	0.2 (-5.2)**	0.7 (-1.7)**
D4	0.3 (-0.1)	0.3 (-1)**	0.3 (-1)**	0.4 (0.4)**
D6	0.4 (-0.1)	0.4 (-1)**	0.4 (-0.4)*	0.4 (-0.1)
D7	0.4 (-0.6)**	0.4 (-1.2)**	0.4 (-0.8)**	0.4 (-0.3)*
MD10	0.4 (-2.6)**	0.1 (-4.5)**	0.2 (-5.4)**	1 (-1.4)**
P8	1.3 (-1.1)**	1.1 (-3.1)**	1.6 (-0.3)*	2.2 (0)

* $p < 0.05$; ** $p < 0.005$